International Journal of Mass Spectrometry 203 (2000) 71–81

Femtosecond laser mass spectroscopy of ferrocenes: Photochemical stabilization by bridged cyclopentadienyl rings?

M. Clara, J.E. Braun, Th. Hellerer, H.J. Neusser*

Institut für Physikalische und Theoretische Chemie, Technische Universität München, D-85748 Garching, Germany

Received 18 May 2000; accepted 29 June 2000

Abstract

We present time-of-flight mass spectra of ferrocene measured with 200 fs UV laser pulses at various wavelengths. As a striking result, strong parent ion peaks and $FeCp^+$ fragments are observed in the femtosecond experiment while in the nanosecond mass spectra only Fe^+ fragment peaks have been detected. The latter is ascribed to a fast dissociation of neutral ferrocene after absorption of the first photon. Excitation with femtosecond pulses favors further photon absorption and ionization. The measured fragmentation patterns are explained by an energetic model assuming switching of absorption from the neutral molecule to the ion as soon as the ionization energy is reached. The bridging of the two Cp rings in [3]-ferrocenophan seems to stabilize the cation but does not suppress the fast production of Fe from electronically excited neutral molecules. (Int J Mass Spectrom 203 (2000) 71–81) © 2000 Elsevier Science B.V.

Keywords: Ferrocenes; Femtosecond excitation; Laser mass spectrometry; Charge transfer; Multiphoton ionization

1. Introduction

The reactivity of organometallic compounds after electronic excitation has attracted great interest. Here, the knowledge of the properties of electronically excited states and the dissociation pathways promises a better understanding of the involved charge-transfer process playing a central role in excited state chemistry.

Ferrocene, [bis(cyclopentadienyl)]Fe(II), $Fe(C_5H_5)_2$, or $Fe(Cp)_2$ (see Fig. 1a), discovered in 1951 [1], is an organometallic sandwich compound of prototype character. Its photophysical properties have been investigated by various groups ([2] and references therein). Some smooth features in the absorption spectrum were assigned to d–d transitions in Fe, metal-to-ligand or ligand-to-metal charge-transfer transitions, and electronic transitions within the cyclopentadienyl (Cp) rings [3]. Because of the more or less structureless absorption bands of gaseous ferrocene with broad peaks [3,4] in the interesting wavelength range <400 nm, precise information about the quantum chemical properties of the molecule, for example, vibrational frequencies or momentum of inertia, cannot be obtained. This can be explained by the large number of vibrational modes (57 internal degrees of freedom) and a high density of electronic states of various multiplicities.

In a series of multiphoton dissociation (MPD)/ multiphoton ionization (MPI) studies of ferrocene [4–11] with nanosecond laser pulses at various wave-

---

* Corresponding author. E-mail: neusser@ch.tum.de

PII S1387-3806(00)00287-6

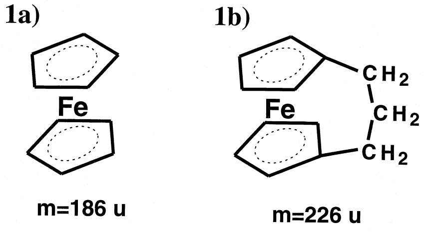

Fig. 1. Ferrocene derivatives investigated in this work: (a) ferrocene; (b) [3]-ferrocenophan.

lengths in the near UV and the visible (UV/VIS), it has been shown that one or both Cp ligands are lost before ionization when a resonant intermediate state is excited in the multiphoton process, and as a consequence, no intact ferrocene cations were observed in the mass spectra. The central Fe atom loses its Cp rings after absorption of one or more UV photons, and the uncharged Fe atom can be ionized and thus detected by resonance-enhanced multiphoton ionization when the laser wavelength is close to an atomic resonance. Recently, we have demonstrated [12] that intact ferrocene cations are produced in a nanosecond experiment when the fast dissociation is bypassed by local excitation and ionization of a ferrocene-aniline derivative. There the aniline acts as a chromophor for photon absorption and, after local ionization, a fast intramolecular charge transfer takes place. The detailed mechanism of photon absorption, energy redistribution, and dissociation in the neutral electronically excited ferrocene has not been unequivocally established. It was concluded that the dynamics of the dissociation process depend on the chosen photon energy as well as on the laser fluence. Nagano et al. [7] concluded that the conversion of electronic to vibrational energy occurs on a faster time scale than a Cp elimination. However, in two earlier publications a fast dissociation mechanism via electronic repulsive states was proposed by Liou et al. [8,9]. Thus, two competing dissociation mechanisms, one via statistical redistribution the other via direct dissociation, are thought to be possible.

From thermochemical studies [13–15] the dissociation energy E_2, for the decomposition of ferrocene into a neutral Fe atom and two Cp radicals is found to be 6.2 eV. Elimination of only one Cp ring requires an energy of $E_1 = 4$ eV [13], which is noticeably more than necessary for removing the remaining second Cp ring.

While resonance-enhanced multiphoton ionization with typical photon energies $h\nu \leq 6.2$ eV failed to produce parent ions, one-photon vacuum ultraviolet (VUV) ionization of ferrocene has lead to intact parent (ferrocene) ions [16–18]. Determination of the ionization energy (IE) of ferrocene by one-photon VUV or electron-impact ionization yielded slightly differing values in the range between 6.61 and 7.15 eV [17–30]. With increasing photon energy, new dissociation channels are opened [16–18]. For example, for a photon energy of 14.76 eV, the ferrocene cation and a ferrocene fragment $Fe(Cp)^+$ were observed in the mass spectrum. For a photon energy higher by 1.77 eV a tiny but interesting mass peak originating from the fragment $(Cp)_2^+$ appears [16]. This could result from a concerted loss of the two ligands from the Fe atom. A further fragmentation channel is observed at a photon energy of 22.55 eV, where the ferrocene looses a complete Cp ring and an acetylene group. In addition, for this high excitation energy a strong Fe^+ ion peak is observed. Energetically, this channel can be opened with an excitation energy between 12.0 and 15.64 eV [11,17–22]. The value of 17.1 eV [31] seems to be too high.

We would like to point out that soft ionization of ferrocene in a two-photon process with *nanosecond* laser pulses is not possible because of its fast dissociation in the intermediate state. Here the question arises if multiphoton ionization with *femtosecond* pulses can compete with the fast dissociation process and if an additional fragmentation pattern that may be observed is similar to that of VUV photoionization experiments. From this one expects information on the origin of the fragments, that is, whether they are produced by *neutral* dissociation channels or by *ion* fragmentation. Another interesting issue concerns the possible influence of a bridge between the two Cp rings on the stability of the ferrocene in electronically excited states.

In this work we present femtosecond multiphoton mass spectra of ferrocene (see Fig. 1a) and a bridged ferrocene derivative ([3]-ferrocenophan; see Fig. 1b) and compare the results with mass spectra obtained with nanosecond laser pulses.

2. Experimental set-up

Nanosecond and femtosecond experiments were performed with different equipment. They differ mainly in the type of laser used and the molecular beam properties.

The experimental setup used for nanosecond mass spectra was described in detail elsewhere [32,33]. Briefly, it consists of a dye laser (LPD 3000; Lambda Physik) yielding light pulses with a bandwidth of ≈0.3 cm^{-1} (FWHM) and a duration of ≈15 ns (FWHM). The dye laser is pumped by a XeCl excimer laser (EMG 1003i, Lambda Physik). The laser beam intersects a skimmed supersonic molecular beam perpendicularly 15 cm downstream from the nozzle orifice. The light pulses overlap in space and time with the gas pulses in the acceleration region of a linear reflecting time-of-flight mass spectrometer [32]. The supersonic jet is obtained by expanding argon carrier gas with a backing pressure of 3 bar into the vacuum with a heated, pulsed (10-Hz repetition rate) valve. The samples of the investigated ferrocenes were heated up to 160 °C in a sample chamber close to the nozzle of the valve. At this temperature, only little thermal decomposition of the investigated ferrocene derivatives takes place. After the experiment, the remaining substances were removed and analyzed by NMR and electron-impact mass spectrometry. No products originating from thermal decomposition could be found. In order to check if sufficient amounts of the substances have been evaporated, mass spectra with sharply focused laser light at the highest available laser power were recorded, thus forcing complete fragmentation of the ferrocene derivatives and detecting the subsequent production of Fe cations. Excitation and ionization of the ferrocene derivatives was achieved in a resonantly enhanced two-photon one-color process. The so-produced cations were accelerated in an electric potential of 1000 V toward the ion reflector, where they were reflected back toward the multichannel plate ion detector. Mass spectra were recorded by a LeCroy transient recorder system (TR8828) and processed in a microcomputer system.

A schematic drawing of the femtosecond set up is shown in Fig. 2. Cold ferrocene molecules in a supersonic molecular beam were produced by expansion of ferrocene vapor through a heated continuous wave nozzle (orifice: 300 μm ∅) into a vacuum chamber. The typical temperature of the nozzle and the reservoir for the substances was 120 °C. Each of the two reservoirs containing ferrocene and [3]-ferrocenophan was separated from the high vacuum by a needle valve. We tried to make sure that the experimental conditions concerning the laser pulse excitation were the same for ferrocene and [3]-ferrocenophan. For this reason we measured ferrocene first and cleaned the nozzle by heating it for 1 h. After this cleaning procedure we measured the [3]-ferrocenophan under the same laser conditions. Any opening of the vacuum chamber necessary for a chemical cleaning of the nozzle would have led to a delay of at least 1 d.

After passing a skimmer with an entrance aperture of 3 mm ∅, the molecules interact with the femtosecond laser pulses of a slightly focused laser beam. The interaction zone of the laser beam and the molecules is placed in the center of the ion optics of a reflectron time-of-flight mass spectrometer [34]. Here the ferrocene molecules are excited and ionized by a UV femtosecond pulse with a variable wavelength between 265 and 236 nm.

The produced ions are accelerated in a repeller field of 400 V/cm (3 cm) toward the ion reflector and hit the multichannel plates (MCP) after reflection. All mass spectra were recorded with a multichannel scaler/averager (Stanford Research Systems, SR 430).

The laser system consists of a commercial Nd:YLF laser-pumped amplifier (Super-Spitfire, Spectra Physics) seeded with an Ar^+ laser-pumped Ti:sapphire laser (Mira Basic, Coherent). The duration of the oscillator pulses at $\lambda=790$ nm is 80 fs (FWHM) and of the amplified pulses 100 fs (FWHM). The pulse widths are monitored with a home-built interferometric autocorrelator with nonlinear photodiode detection

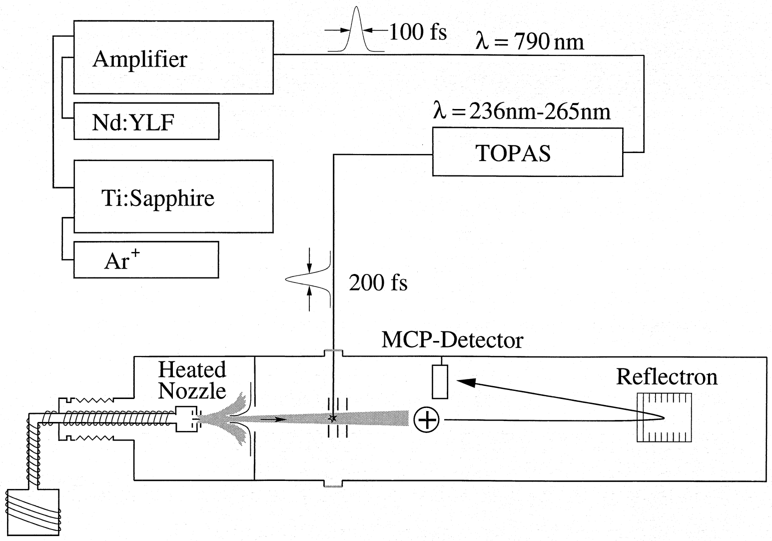

Fig. 2. Scheme of the experimental set-up for the femtosecond ionization experiment in a skimmed cold molecular beam with mass analysis in a reflecting time-of-flight mass spectrometer. The amplified femtosecond light pulses are frequency converted in a TOPAS system leading to UV pulses of 200 fs (FWHM) duration. For details, see text.

[35]. The amplified light beam is directed into a traveling-wave optical parametric amplifier of superfluorescence (TOPAS, Light Conversion), where it pumps parametric processes: After production and amplification of superfluorescence light in a nonlinear crystal, it is mixed with the pump beam in a BBO crystal by sum frequency mixing. The so-produced visible light pulses (460–560 nm) are frequency-doubled in another BBO crystal. The measurements of the UV pulse characteristics are published elsewhere [36]. The pulse duration is 200 fs for the UV pulses, about twice the value of the visible pulses, and can be explained by the length of the doubling crystal used in the experiment.

3. Results and discussion

3.1. Nanosecond-laser mass spectra of ferrocene

The mass spectrum of ferrocene obtained by resonance-enhanced two-photon ionization with nanosecond laser pulses is shown in Fig. 3a. There is no parent ion peak at 186 U, and the pattern does not change for different laser pulse energies. The strong signal at 56 U is assigned to the Fe^+ ion by its typical isotopic pattern [4–11].

The small peak at 114 U results from para-difluorobenzene, which we used for calibration of the mass spectra.

Two possible pathways for the loss of Cp ligands in neutral ferrocene have been discussed [10]:

Photon absorption followed by *concerted*, multiligand loss:

$$Fe(Cp)_2 + nh\nu \rightarrow Fe + 2Cp; \tag{1}$$

Sequence of photon absorption and ligand elimination steps:

$$Fe(Cp)_2 + nh\nu \rightarrow Fe(Cp) + Cp, \tag{2}$$

$$Fe(Cp) + nh\nu \rightarrow Fe + Cp. \tag{3}$$

Both channels lead to an efficient production of neutral Fe. The ionization of the resulting Fe is very efficient for wavelengths in resonance with electronic transition in the Fe atom. This is the case for the wavelength of 248.3 nm used in the mass spectrum of Fig. 3a and in [12], showing a strong Fe^+ peak.

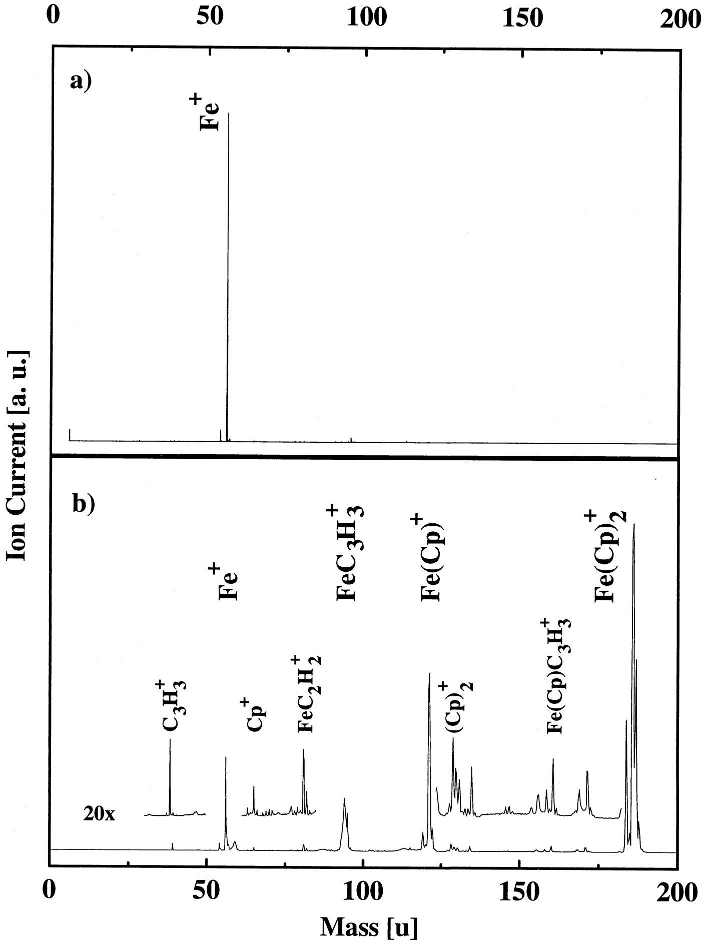

Fig. 3. Multiphoton mass spectra of ferrocene recorded for different laser pulse durations. Excitation with (a) nanosecond laser pulses at 248.3 nm, (b) femtosecond laser pulses at 244 nm. The intensity scale of the inset is magnified by a factor of 20.

3.2. Femtosecond-laser mass spectra of ferrocene

The resonance-enhanced multiphoton mass spectrum of ferrocene resulting from excitation with femtosecond pulses at a wavelength of 244 nm (Fig. 3b) shows a pattern different from that of the mass spectra after nanosecond pulse excitation (Fig. 3a). Here the strongest mass peak is from the parent ion at 186 U and reflects the well-known isotopic pattern of ferrocene. This is mainly given by the isotopic pattern of Fe, only the signal at 187 U is enhanced by the natural abundance of the ^{13}C isotope. Three additional strong mass peaks are detected at 121, 95, and 56 U. The peaks at 121 and 95 U are assigned to $Fe(Cp)^+$ and $FeC_3H_3^+$, respectively. In addition, Fe^+ (56 U) ions are leading to a relatively strong signal. The other smaller peaks at 160, 130, 82, 65, and 39 U are assigned to $Fe(Cp)C_3H_3^+$, $(Cp)_2^+$, $FeC_2H_2^+$, Cp^+, and $C_3H_3^+$, respectively. This is in contrast to the UV femtosecond experiments in [37], with 500-fs laser pulses and CO_2 laser evaporation where only parent ions (ferrocene cation) were observed.

The most plausible explanation for the appearance of the strong parent peak is the fast sequential absorption of two photons during the short femtosecond pulses. Obviously, in this case the second photon is absorbed before a dissociation can take place in the intermediate state.

As demonstrated above, the production of *neutral* Fe in the intermediate state with subsequent multiphoton ionization is the dominant process in the nanosecond experiment leading to strong Fe^+ peaks. This channel can be also active in the femtosecond experiment; however, it happens with much lower efficiency. Another possible pathway for Fe^+ production is a fragmentation of the ferrocene cation, which will be discussed below.

To check if the production of $FeCp^+$ originates from a dissociation in the neutral ferrocene with subsequent ionization of the FeCp product or from a fragmentation in the ferrocene cation, we measured the intensity dependence of the ion signals. With increasing laser intensity the ferrocene cation signal is decreasing, whereas the Fe^+ and $FeCp^+$ ion signals are increasing at the same time. These results indicate that multiphoton fragmentation of the parent cation is the dominant process for production of fragment ions in the case of ferrocene, like in the case of $Fe(CO)_5$ for high laser intensities [38]. The production of neutral Fe occuring from the fast dissociation of ferrocene in the neutral intermediate state seems to be have minor importance but cannot be excluded.

Next, we would like to explain the fragmentation pattern observed in Fig. 3b by considering the energetics of different fragmentation channels of the ferrocene parent cation (see Fig. 4). We assume that after ionization of ferrocene, take-up of energy is possible by photon absorption within the parent ion. The absorption of further photons within the neutral molecule above the IE could also occur via long-lived autoionization resonances, but it appears to be less efficient for the 200-fs pulses used in this work. We assumed that the fast direct ionization is the dominating channel and that the absorption takes place in the parent ion as soon as the ionization energy is reached [39].

To trace out an energetic model, the appearance energies for several ferrocene fragments measured by other groups with various techniques are listed in Table 1. The values for the ionization and the appearance energies of the different ionic fragments in the literature were obtained by VUV single-photon ionization [17,18] and electron impact [19–22,31,40]. We would like to point out that in the cited experiments the energy leading to an ionization or a fragmentation was deposited in the ferrocene molecules in a single step. In the multiphoton experiment of this work the energy take-up occurs in a different way, leading to the same internal energy but not necessarily to the same originally excited state. From the known data we conclude the following excitation/dissociation pathways illustrated in Fig. 4: first, after absorption of two photons in the neutral ferrocene a prompt ionization process occurs leading to the production of ferrocene parent ions with an unknown amount of internal energy because part of the excess energy of 3.4 eV above the IE is carried away by the electron as kinetic energy. Second, the parent ion absorbs further photons. If the internal energy of the ferrocene ion is >1.5–2 eV, the absorption of one photon with an energy of 5.08 eV is sufficient to energetically open the lowest fragmentation channels of the ferrocene ion (see Table 1).

$$Fe(Cp)_2^+ + h\nu \rightarrow Fe(Cp)^+ + Cp, \qquad (4)$$

$$Fe(Cp)_2^+ + h\nu \rightarrow (Cp)_2^+ + Fe, \qquad (5)$$

$$Fe(Cp)_2^+ + h\nu \rightarrow Fe(Cp)C_3H_3^+ + C_2H_2, \qquad (6)$$

$$Fe(Cp)_2^+ + h\nu \rightarrow Fe^+ + 2Cp. \qquad (7)$$

The products $Fe(Cp)^+$, $(Cp)_2^+$, $Fe(Cp)C_3H_3^+$, and Fe^+ are indeed observed in our mass spectrum. However, the small excess energy after absorption of one photon would lead to a very slow decay process [41] and, therefore, we expect that a second photon is absorbed before these dissociation channels lead to a microsecond decay within the acceleration region of the mass spectrometer. Therefore, it is more likely that at least two photons are absorbed in the ferrocene cation before dissociation takes place. New fragment channels can be opened at this high excitation energy (see Table 1):

$$Fe(Cp)_2^+ + 2h\nu \rightarrow FeC_3H_3^+ + Cp + C_2H_2; \qquad (8)$$

$$Fe(Cp)_2^+ + 2h\nu \rightarrow FeC_2H_2^+ + Cp + C_3H_3. \qquad (9)$$

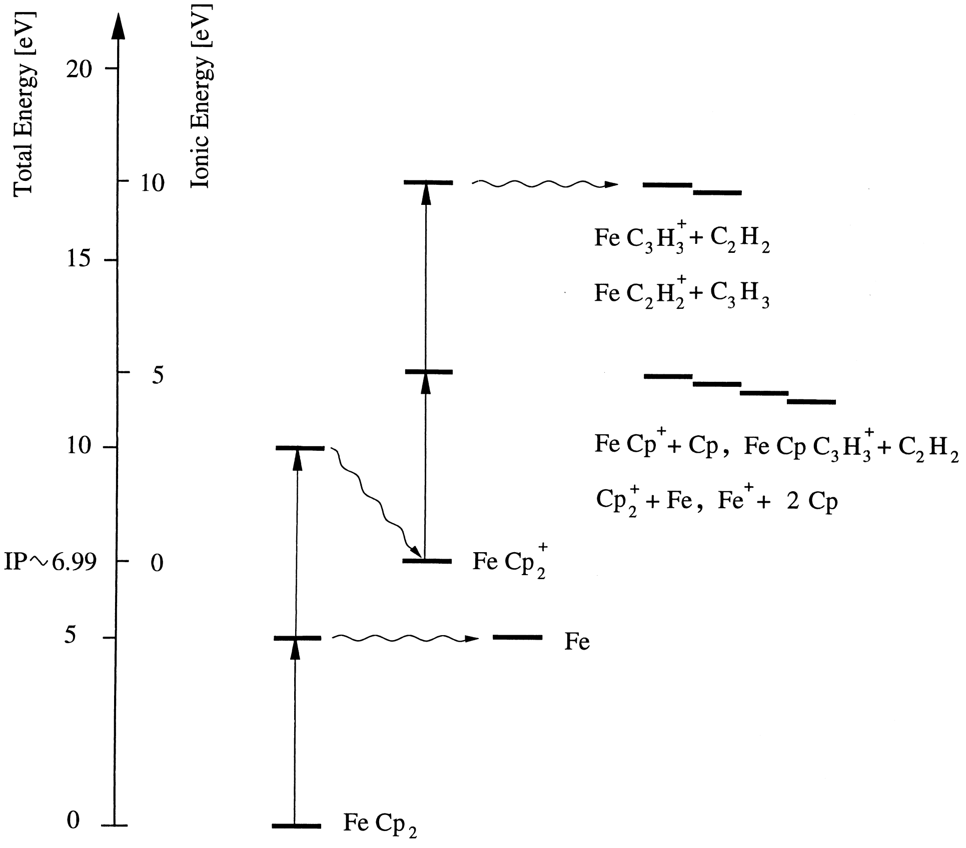

Fig. 4. Energetic scheme for excitation of ferrocene with femtosecond laser pulses. The indicated fragmentation channels of the ferrocene parent cation are found from energetic considerations.

All fragments are indeed observed in the mass mass spectrum of Fig. 3b. The dominant signal is the ferrocene ion peak. This means that there is a small probability for the absorption of additional photons within the parent ion after its production, probably because of the small absorption cross section at the given wavelength. The second dominant peak at 121 U is assigned to $Fe(Cp)^+$. The Cp loss channel (Eq. (4)) is stronger than the $(Cp)_2^+$ (Eq. (5)), $Fe(Cp)C_3H_3^+$ (Eq. (6)), and Fe^+ (Eq. (7)) fragment channels, though the energetic thresholds for the latter are lower. The reason for this might be a faster rate of the Cp elimination channel because of entropic reasons, that is, a higher density of states. No indication of a metastable decay is observed.

Table 1
Values for the appearance energy of fragment ions of ferrocene taken from the literature

Fragment	Appearance Energy
$Fe(Cp)^+$	13.3,[a] 13.9,[b] 12.8,[c] 13.78,[d] 11.6,[e] 13.162,[f] 13.93,[g] 12.95,[h] 14.38,[i]
$(Cp)_2^+$	13.5,[a] 13.96[g]
$Fe(Cp)C_3H_3^+$	13.2,[a] 13.27[d]
Fe^+	14.3,[a] 12.0,[b] 14.4,[d] 15.64,[e] 13.506,[f] 14.0,[g] 14.1,[h] 17.1[i]
$FeC_3H_3^+$	17.5,[a] 18.9,[d] 18.06,[g] 17.75[h]

[a] Ref. [18]. [b] Ref. [19]. [c] Ref. [40]. [d] Ref. [22]. [e] Ref. [11]. [f] Ref. [17]. [g] Ref. [20]. [h] Ref. [21]. [i] Ref. [31]

Finally, we would like to compare the mass spectrum of the femtosecond experiment with the typical mass pattern measured in VUV photoionization [16]. As discussed above, the way the energy is deposited in the system is totally different in the two types of experiments but the total energy might be same. In the VUV experiment the energy is deposited in the system in a single step, while in the femtosecond experiment photon absorption takes place first in the neutral molecules and then in the parent ion after its production. Here the question arises whether the different excitation pathways lead to different mass pattern. A comparison of the mass pattern in Fig. 3b with the mass spectra of [16] shows the same peaks with a comparable intensity distribution. This means that the fragmentation pattern recorded with 20 eV photon energy is basically the same as that achieved with multiphoton absorption of 5.08 eV photons with femtosecond laser pulses. In particular, the intensity of the Fe^+ ion signal is the same for both experiments. This is a strong indication for the production of Fe^+ ions in a fragmentation process of the ferrocene cation. This corroborates our assumption that the femtosecond fragmentation patterns originates from ionic fragmentation channels after a total of four photons has been absorbed leading to a total energy of ~20 eV. The similarity of the mass pattern shows that only the total amount of energy is important, as is expected for a statistical dissociation process.

The appearance of a $C_3H_3^+$ ion signal is another interesting detail of the measured mass spectrum. Complementary to the elimination of an acetylene group (Eq. (8)) where the larger fragment $FeC_3H_3^+$ carries the charge, it seems to be possible that the charge remains at the smaller C_3H_3 fragment after a separation process caused by the relatively small ionization energy (see Table 2). Here a comparison with the VUV spectra of [16] is not possible because the published VUV mass spectrum does not show the weak features.

3.3. Mass spectra of bridged ferrocene

3.3.1. Nanosecond mass spectra

The simplest bridged ferrocene is [3]-ferrocenophan (see Fig. 1b). A C_3H_6 bridge constitutes a connecting link between the two cyclopentadienyl rings that could lead to a stabilization of neutral [3]-ferrocenophan in its electronically excited states so that a soft ionization of [3]-ferrocenophan should become possible in a nanosecond experiment as well.

Table 2
Values for the ionization energy of ferrocene and some of its fragments taken from the literature

Neutral Fragment	Ionization Energy (eV)
$Fe(Cp)_2$	6.82,[a] 6.61,[b] 6.9,[b] 6.747,[c] 6.9,[d] 6.72,[e] 6.75,[f] 6.78,[g] 6.9,[h] 7.15,[i] 6.97,[j] 6.99,[k] 6.86,[l] 6.88,[m,n] 6.99[o]
Fe	7.78
C_3H_3	6.6[p]
C_2H_2	11.4[q]
Cp	8.41,[q] 8.56,[r] 8.69[s]
$Fe(C_5H_4)_2C_3H_6$	6.66[t]

[a] Ref. [23]. [b]Ref. [18]. [c]Ref. [17]. [d]Ref. [19]. [e]Ref. [24]. [f]Ref. [20]. [g]Ref. [25]. [h,i]Ref. [21,22]. [j]Ref. [26]. [k]Ref. [27]. [l]Ref. [28]. [m,n,o]Ref. [29,30,11]. [p,q,r,s]Ref. [50]. [t]Ref. [43,44].

The spectroscopic properties of [3]-ferrocenophan have not yet been investigated. Its ionization energy was measured by Vondrak [42] and Al-Saeed et al. [44] using VUV photoelectron spectroscopy (He I), and it was found that the vertical IE of [3]-ferrocenophan is very close to that of ferrocene (see Table 2). The structure and chemistry of bridged ferrocenes was investigated by Rosenblum et al. [44]. The UV absorption spectra of ferrocene and [3]-ferrocenophan are not very different, and the sublimation temperature is comparable to that of ferrocene.

First, we investigated the [3]-ferrocenophan with nanosecond laser pulses under the same experimental conditions as for ferrocene. We found no difference between the mass spectrum of [3]-ferrocenophan and the mass spectrum of ferrocene (see Fig. 2a); that is, both are dominated by the strong Fe^+ peak and no parent ion peaks appear. Also, the wavelength dependence of the mass spectra is the same. This demonstrates that there is basically no effect of the bridging on the stability of [3]-ferrocenophan in the neutral electronically excited intermediate state.

3.3.2. Femtosecond mass spectra

In Fig. 5 the mass spectrum is shown when recorded with femtosecond laser pulses. The mass pattern differs from that in the nanosecond experiments like in the case of ferrocene. The [3]-ferro-

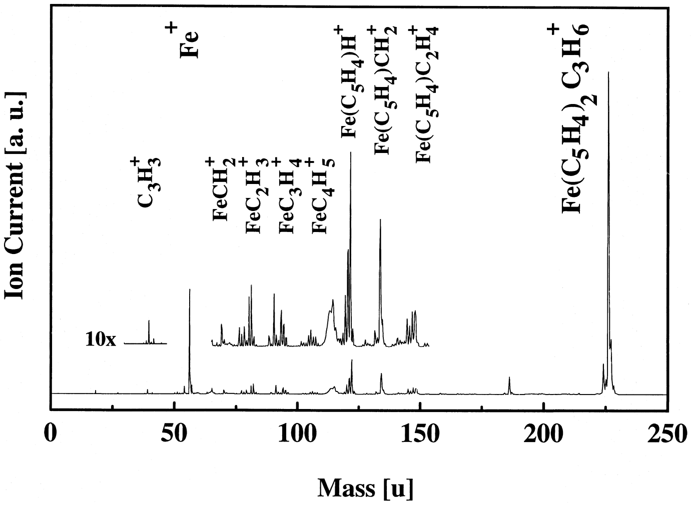

Fig. 5. Multiphoton mass spectra of [3]-ferrocenophan recorded with femtosecond laser pulses at 244 nm. The intensity scale of the inset is magnified by a factor of 10.

cenophan parent ion at 226 U is the prominent feature and displays the expected typical isotopic pattern. This is what we expect from the femtosecond results for ferrocene, and it means that a soft two-photon ionization of this organometallic compound is possible with femtosecond laser pulses.

The second dominant peak at 56 U is assigned to Fe$^+$. As described above for the case of ferrocene, a fragmentation of ionic [3]-ferrocenophan leads directly to Fe$^+$. In addition, a great number of smaller peaks is detected in the femtosecond laser experiment of [3]-ferrocenophan. There is a peak at 186 U that is an artefact caused by traces of ferrocene in the nozzle (see Section 2). An amount of $<$5% is acceptable and does not lead to a perturbation of the fragment spectrum of [3]-ferrocenophan. There is a common feature of all other signals: All fragments of [3]-ferrocenophan are showing an H loss fragmentation pattern with a mass difference of the individual peaks of just a few units. The largest fragment at 148 U is assigned to $Fe(C_5H_4)C_2H_4^+$. This is a fragment typical for the breaking of the bridge. The three neighbored peaks are assigned to H loss channels. In addition, we assign the fragment at 134 U ($Fe(C_5H_4)CH_2^+$) as caused by the breaking of the bridge at another C–C bond. Again, the neighbored peaks at smaller masses result from H loss channels. There is a third fragment with an H loss pattern at 122 U, assigned to $Fe(C_5H_4)H^+$.

Another group of fragments can be found by their common fragmentation mechanism: Here the bond breaking takes place inside a Cp ring leading to an Fe atom bound to a Cp ring fragment. The peak with the largest mass is relatively small and assigned to $FeC_4H_5^+$ (109 U) with a typical H loss pattern. The peaks at 96, 83, and 70 U with H loss patterns are assigned to $FeC_3H_4^+$, $FeC_2H_3^+$, and $FeCH_2^+$, respectively.

The smallest fragment ion of the [3]-ferrocenophan is $C_3H_3^+$ (39 U), as in the case of ferrocene. The mechanism for the production of this small fragment is probably the same as for the case of ferrocene (see above).

3.3.3. Comparison with ferrocene mass spectra

There are a couple of differences between the fragmentation pattern of ferrocene and [3]-ferrocenophan in the femtosecond mass spectra: The dominant fragmentation pathway of the ferrocene cation (see Fig. 3b) is the loss of a Cp ring and the subsequent separation of an acetylene group. No dominant fragment of [3]-ferrocenophan comparable to the $Fe(Cp)^+$ in the case of ferrocene is observed. This means that this fragmentation channel (see Eq. (4)) is hindered by the bridge. As we found a clear difference in the fragmentation behavior for the ferrocene and [3]-ferrocenophan *cations*, we conclude that the opening of the lowest fragmentation channels of the [3]-ferrocenophan requires a much higher energy than in the case of ferrocene. This is caused by the bridging of the two Cp rings. In addition to the bond breaking between the Fe and a Cp ring that takes >4 eV (see Tables 1, 2 for ferrocene), the necessary breaking of the C–C bond in the bridge requires ~ 3.6 eV. No special fragment seems to be prefered energetically.

4. Summary and outlook

In this article, we presented TOF mass spectra of ferrocene and [3]-ferrocenophan resulting from ionization with UV nanosecond laser pulses and with UV femtosecond laser pulses. In the nanosecond experiment, ferrocene is excited to an intermediate electronic state, and then a fast dissociation process occurs. Neutral Fe is produced before the absorption of a second photon leads to the ionization of ferrocene. Fe can be ionized very easily if the laser frequence is in resonance with an atomic transition of Fe leading to a strong Fe^+ signal in the mass spectra, but no parent signal is found. The result is completely different for the multiphoton femtosecond laser mass spectra. Here the strongest peaks are produced by intact ferrocene ions and many other molecular fragment ions larger than Fe^+ appear. From that we conclude that after absorption of two photons the ferrocene is promptly ionized and, after absorption of one or two further photons, various fragmentation channels of the ferrocene parent cation are open.

To check the influence of a bridging of the two Cp rings on the neutral dissociation and on ion fragmentation behavior we also investigated the [3]-ferrocenophan. Here the two Cp rings are linked by a C_3H_6 bridge. We found no difference in the nanosecond laser mass spectra of this derivative and $Fe(Cp)_2$. This strongly indicates that there is no stabilization of the intermediate state by the bridge. However, the mass spectra recorded with femtosecond laser pulses differ for both molecules. The mass spectrum of ferrocene is dominated by the parent ion. In addition, an Fe^+ peak and two further relatively strong mass peaks appear. The latter can be assigned to $Fe(Cp)^+$ and $FeC_3H_3^+$, resulting from an fragmentation of the ferrocene ion. In the case of [3]-ferrocenophan the femtosecond mass spectrum is dominated by the parent ion and Fe^+ peaks alone without further fragments. Obviously, here a stabilization of the [3]-ferrocenophan ion is caused by the bridge and hinders fragmentation of the ion.

We compared the mass pattern of ferrocene recorded with UV femtosecond laser pulses with previous VUV photoionization measurements. No basic differences were found. Though the internal energy is comparable in both cases if four photons are absorbed in the femtosecond experiment, it is deposited in a different way. In the VUV experiment a direct one-photon ionization is performed, whereas in the femtosecond experiments four photons are absorbed via resonant intermediate states. From the experimental finding that the fragmentation patterns are nearly identical in both cases, we conclude that a complete redistribution of the internal energy takes place in both cases before ionic fragmentation and the dissociation occurs according to a statistical decay process [45].

Here the interesting question arises of whether the fragmentation behavior of the ferrocene cation observed in the femtosecond experiment can be influenced by suitable pulse shaping of the femtosecond pulses. Recently, this was demonstrated for $Fe(CO)_5$ and $CpFe(CO)_2Cl$ in an experiment with feedback-optimized phase-shaped femtosecond laser pulses [46]. The optimization of special reaction paths using the coherence of lasers was proposed theoretically by Brumer and Shapiro [48]. Tannor, and Rice [48] suggested a control of chemical reaction via control of wave packet evolution by a pump-probe technique.

Acknowledgements

We thank P. Härter for supplying the metallorganic components and Alexander Genest for his assistance. Financial support from the Deutsche Forschungsgemeinschaft (Schwerpunktprogramm: Femtosekunden-Spektroskopie elementarer Anregungen in Atomen, Molekülen und Clustern) and the Fonds der Chemischen Industrie are gratefully acknowledged.

References

[1] T.J. Kealey, P.L. Pauson, Nature 168 (1951) 1039.
[2] A. Togni, T. Hayashi, Ferrocenes, 1995.
[3] A.T. Armstrong, F. Smith, E. Elder, S.P. McGlynn, J. Chem. Phys. 46 (1967) 4321.
[4] S. Leutwyler, U. Even, J. Jortner, J. Phys. Chem. 85 (1981) 3026.
[5] S. Leutwyler, U. Even, J. Jortner, Chem. Phys. Lett. 74 (1980) 11.
[6] P.C. Engelking, Chem. Phys. Lett. 74 (1980) 207.
[7] Y. Nagano, Y. Achiba, K. Kimura, J. Phys. Chem. 90 (1986) 1288.
[8] H.T. Liou, Y. Ono, P.C. Engelking, J.T. Moseley, J. Phys. Chem. 90 (1986) 2888.
[9] H.T. Liou, P.C. Engelking, Y. Ono, J.T. Moseley, J. Phys. Chem. 90 (1986) 2892.
[10] U. Ray, H.Q. Hui, Z. Zhang, W. Schwarz, M. Vernon, J. Chem. Phys. 90 (1989) 4248.
[11] J. Opitz, P. Härter, Int. J. Mass. Spec. Ion. Processes 121 (1992) 183.
[12] J.E. Braun, H.J. Neusser, P. Härter, M. Stöckl, J. Phys. Chem. 104 (2000) 2013.
[13] K.E. Lewis, G.P. Smith, J. Am. Chem. Soc. 106 (1984) 4650.
[14] J.A. Connor, Top. Curr. Chem. 71 (1977) 71.
[15] G. Wilkinson, P.L. Pauson, F.A. Cotton, J. Am. Chem. Soc. 76 (1954) 1970.
[16] S.-J. Han, M.C. Yang, C.H. Hwang, D.H. Woo, J.R. Hahn, H. Kang, Y. Chung, Int. J. Mass. Spec. 181 (1998) 59.
[17] R. Bär, Th. Heinis, Ch. Nager, M. Jungen, Chem. Phys. Lett. 91 (1982) 440.
[18] S. Barfuss, K.-H. Emerich, W. Hirschwald, P.A. Dowben, N.M. Boag, J. Org. Chem. 391 (1990) 209.
[19] G.M. Begun, R.N. Compton, J. Chem. Phys. 58 (1973) 2271.
[20] G.D. Flesch, G.A. Junk, H.J. Svec, J. Chem. Soc. Dalton Trans. 11 (1972) 1102.
[21] J.-P. Puttemans, A. Hanson, Ing. Chim. 53 (1971) 17.
[22] J. Muller, L. D’Or, J. Organometal. Chem. 10 (1967) 313.
[23] M.F. Ryan, J.R. Eyler, D.E. Richardson, J. Am. Chem. Soc. 114 (1992) 8611.
[24] J.W. Rabalais, L.O. Werme, T. Bergmark, L. Karlsson, M. Hussain, K. Siegbahn, J. Chem. Phys. 57 (1972) 1185.
[25] V.K. Adamchuk, A.B. Dmitriev, G.V. Prudnikova, L.S. Sorokin, Opt. Spectrosc. 33 (1972) 191.
[26] G. Huttner, E.O. Fischer, J. Organometal. Chem. 8 (1967) 299.
[27] A. Foffani, S. Pignataro, G. Distefano, G. Innorta, J. Organometal. Chem. 7 (1967) 473.
[28] C. Cauletti, J.C. Green, M.R. Kelly, P. Powell, J. van Tilborg, J. Robbins, J. Smart, J. Electron Spectrosc. Relat. Phenom. 19 (1980) 327.
[29] S. Evans, M.L.H. Green, B. Jewitt, A.F. Orchard, C.F. Pygall, J. Chem. Soc. Faraday Trans. 68 (1972) 1847.
[30] S. Evans, M.L.H. Green, B. Jewitt, G.H. King, A.F. Orchard, J. Chem. Soc. Faraday Trans. 70 (1974) 356.
[31] L. Friedman, A.P. Irsa, G. Wilkinson, J. Am. Chem. Soc. 77 (1955) 3689.
[32] B. Ernstberger, H. Krause, A. Kiermeier, H.J. Neusser, J. Chem. Phys. 92 (1990) 5285.
[33] Th. L. Grebner, B. Ernstberger, H.J. Neusser, Int. J. Mass Spectrom. Ion Processes 136 (1994) 101.
[34] U. Boesl, H.J. Neusser, R. Weinkauf, E.W. Schlag, J. Phys. Chem. 86 (1982) 4857.
[35] Th. Hellerer, Diplomarbeit, Technische Universität München, 1999.
[36] M. Clara, Th. Hellerer, H.J. Neusser, Appl. Phys. B 71 (2000) 431.
[37] C. Grun, C. Weickhardt, J. Grotemeyer, Eur. Mass Spectrom. 2 (1996) 197.
[38] L. Banares, T. Baumert, M. Bergt, B. Kiefer, G. Gerber, J. Chem. Phys. 108 (1998) 5799.
[39] W. Dietz, H.J. Neusser, U. Boesl, E.W. Schlag, S.H. Lin, Chem. Phys. 66 (1982) 105.
[40] S. Pignataro, F.P. Lossing, J. Organometal. Chem. 10 (1967) 531.
[41] W. Forst, Theory of Unimolecular Reactions, Academic Press, New York, 1973.
[42] T. Vondrak, Polyhedron 4 (1985) 1271.
[43] A.M. Al-Saeed, E.A. Seddon, K.R. Seddon, A.A. Shimran, S. Tompkins, M.C. Grossel, J.P. Knychala, J. Organometal. Chem. 347 (1988) C25.
[44] M. Rosenblum et al, J. Am. Chem. Soc. 85 (1963) 316.
[45] R.A. Marcus, O.K. Rice, J. Phys. Colloid. Chem. 55 (1951) 894.
[46] A. Assion, T. Baumert, M. Bergt, T. Brixner, B. Kiefer, V. Seyfried, M. Strehle, G. Gerber, Science 282 (1998) 919.
[47] P. Brumer, M. Shapiro, Chem. Phys. Lett. 126 (1986) 541.
[48] D.J. Tannor, S.A. Rice, J. Chem. Phys. 83 (1985) 5013.
[49] http://webbook.nist.gov.